Contribution from Ames Laboratory—DOE[1] and the Department of Chemistry, Iowa State University, Ames, Iowa 50011

Alkali-Metal Intercalates of Layered Yttrium Chloride Oxide and Their Hydration Reactions

JEFF E. FORD and JOHN D. CORBETT*

Received March 29, 1985

Reactions of M^ICl, M^I = Li–Cs, with Y and YCl_3–Y_2O_3 or YOCl at ~950 °C give high yields of layered M^I_xYClO with three types of structures: 3R for Li–Cs, 2H for Na–Cs, and 1T for Cs. Only the 3R (and 1T-Cs) phases are formed in a presumably concerted process when YOCl (PbFCl type) is the reactant. The 3R- and 1T-type phases are nonstoichiometric in alkali-metal content and are favored by higher MCl concentrations, with $\sim 0.1 < x \leq \sim 0.25$ for 3R-K_xYClO. The structures of 2H-K_xYClO and 3R-Na_xYClO were established with single crystals formed in melt reactions with adventitious oxygen. The space groups, lattice constants, refined R and R_w, and M^I and O occupancies are as follows. 2H-K_xYClO: $P6_3/mmc$, a = 3.7873 (6) Å, c = 21.860 (8) Å, 0.057, 0.075, 0.08 (6), 0.82 (6). 3R-Na_xYClO: $R\bar{3}m$, a = 3.7881 (3) Å, c = 29.445 (5) Å, 0.109, 0.122, 0.08 (3), 1.0 (1). The coordination of the alkali metal is trigonal antiprismatic in the 3R type and trigonal prismatic in the 2H and 1T types. The 3R form is oxidized by I_2 in CH_3CN to samples of well-crystallized YOCl in the new YOF-type structure. The 3R phase may be thus viewed as the intercalate of either YOCl in the YOF-type structure or a derivative of 3R-YCl with oxygen in all tetrahedral holes. Moist air reversibly hydrates the 3R-K and -Rb (but not -Li) phases and the 2H-Rb salt with coherent conversion of the former to a 1T-type structure analogous to 1T-Cs_xYClO. Liquid water oxidizes and exfoliates the 3R phases but is without effect on 2H samples. These results are compared with those for the analogous transition-metal disulfide compounds.

Introduction

The novel structures reported for the monohalides ZrCl,[2] ZrBr,[3] ScCl,[4] and YCl[5,6] as well as those of many lanthanide elements[7] all provide basically a two-dimensional metallike substrate for study. Their structures consist of alternating pairs of cubic-close-packed metal and chlorine or bromine layers, which bond to give tightly bound slabs with the layers sequenced X–M–M–X and oriented AbcA. These slabs are in turn weakly bound by van der Waals type interactions in the order ABC... (designating the outer halogen layers only) in ZrCl, etc., or ACB... in ZrBr, HfCl, ScCl, YCl, and so forth. Strong bonding of the double metal layers by three electrons per metal in ZrX, for example, produces two-dimensional and evidently metallic compounds.

In recent years a variety of interstitial derivatives of these monohalides have been discovered in which a light atom is bound between the double metal layers. The zirconium phases react reversibly with hydrogen at room temperature to ~450 °C to form first $ZrXH_{0.5}$ and subsequently ZrXH.[8] In $ZrXH_{0.5}$ and ZrXH, four-layer slabs are retained but reordered, and the hydrogen is inserted in the nominal tetrahedral interstices defined by the metal atoms in the former[9] but in pairs in the so-called octahedral sites in the latter.[10] On the other hand, the monohalide hydrides of scandium, yttrium, lanthanum, and gadolinium retain ZrX type structures with hydrogen in tetrahedral sites.[11-14] The zirconium monohalides also react with ZrO_2 at ~980 °C without a phase change to form $ZrXO_y$ phases where oxygen is bound in the (flattened) tetrahedral holes between the double metal layers.[15] Carbides M_2Cl_2C, M = Sc, Y,[16] Zr,[17] and Gd,[11] are also known, now with occupancy of the nominal octahedral sites. The light-atom interstitial compounds are not limited to the monohalide-based phases but also occur in other types of compounds, for example, recently discovered carbides such as $Sc_7Cl_{10}C_2$,[18] Gd_3Cl_3C,[19] and $Gd_5Cl_9C_2$.[20]

The intercalation of guest species into a host lattice is another familiar type of reaction for many layered materials.[21,22] Compounds of this type are well-known for the layered dichalcogenides and other phases but only recently for intercalated halides, namely, with $Li_{0.2}YCl$ and $Li_{0.5}GdCl$.[6,14] In these the lithium is, respectively, randomly distributed in 40% of or is occupying all of the trigonal-antiprismatic sites between the chlorine layers of typical monohalide slabs. On the other hand, the synthesis of the analogous derivatives of ZrX has to date not succeeded.[15]

The present article reports the synthesis of what can be viewed as alkali-metal intercalation compounds either of the oxygen interstitial derivatives of YCl analogous to the $ZrXO_y$ phases noted above but with substantially full oxygen occupancy, viz. M^I_xYClO, or of an otherwise metastable layered (YOF type) form of YOCl.[23] These materials are obtained from high-temperature reactions of M^ICl, Y, and either YCl_3–Y_2O_3 or YOCl. A wide range of phases for M^I = Li–Cs in three different structure types has been identified with the aid of Guinier powder photographs, the structure of two types being established by a single-crystal X-ray study of one member of each. The latter are among the very few examples of simple layered intercalates obtained that are well enough crystallized to allow structural characterization by single-crystal X-ray diffraction means.

Experimental Section

Syntheses. The air and moisture sensitivity of the reactants and products even at room temperature dictates the use of typical drybox and

(1) Operated for the U. S. Department of Energy by Iowa State University under Contract No. W-7405-Eng-82. This research was supported by the Office of Basic Energy Sciences, Materials Sciences Division.
(2) Adolphson, D. G.; Corbett, J. D. *Inorg. Chem.* **1976**, *15*, 1820.
(3) Daake, R. L.; Corbett, J. D. *Inorg. Chem.* **1977**, *26*, 2029.
(4) Poeppelmeier, K. R.; Corbett, J. D. *Inorg. Chem.* **1977**, *16*, 1109.
(5) Mattausch, Hj.; Hendricks, J. B.; Eger, R.; Corbett, J. D.; Simon, A. *Inorg. Chem.* **1980**, *19*, 2128.
(6) Ford, J. E.; Meyer, G.; Corbett, J. D. *Inorg. Chem.* **1984**, *23*, 2094.
(7) Mattausch, Hj.; Simon, A.; Holzer, N.; Eger, R. *Z. Anorg. Allg. Chem.* **1980**, *466*, 7.
(8) Struss, A. W.; Corbett, J. D. *Inorg. Chem.* **1977**, *16*, 360.
(9) Marek, H. S.; Corbett, J. D.; Daake, R. L. *J. Less-Common Met.* **1983**, *89*, 243.
(10) Wijeyesekera, S. D.; Corbett, J. D. *Solid State Commun.* **1985**, *54*, 657.
(11) Simon, A. *J. Solid State Chem.* **1985**, *57*, 2.
(12) Ueno, F.; Ziebeck, K.; Mattausch, Hj.; Simon, A. *Rev. Chim. Miner.* **1984**, *21*, 804.
(13) Wijeyesekera, S. D.; Hwu, S.-J.; Corbett, J. D., to be submitted for publication.
(14) There is now good evidence that perhaps all of the reported rare-earth-element monohalides and their intercalates may actually exist only when stabilized by some amount of interstitial hydrogen, this having originated at first as an impurity.[11,13]
(15) Seaverson, L. M.; Corbett, J. D. *Inorg. Chem.* **1983**, *22*, 3202.
(16) Ziebarth, R. P.; Corbett, J. D., unpublished research, 1983.
(17) Ford, J. E.; Hwu, S.-J.; Corbett, J. D. *Inorg. Chem.* **1983**, *22*, 2789.
(18) Hwu, S.-J.; Corbett, J. D.; Poeppelmeier, K. R. *J. Solid State Chem.* **1985**, *57*, 43.
(19) Warkentin, E.; Simon, A. *Rev. Chim. Miner.* **1983**, *20*, 488.
(20) Warkentin, E.; Masse, R.; Simon, A. *Z. Anorg. Allg. Chem.* **1982**, *491*, 323.
(21) Whittingham, M. S.; Jacobson, A. J. "Intercalation Chemistry"; Academic Press: New York, 1982.
(22) Lévy, F., Ed. "Intercalated Layered Materials"; D. Reidel Publishing Co.: Boston, MA, 1979.
(23) Garcia, E.; Corbett, J. D.; Ford, J. E.; Vary, W. J. *Inorg. Chem.* **1985**, *24*, 494.

0020-1669/85/1324-4120$01.50/0

vacuum line techniques. The dryboxes were constantly purged with dry N_2 that recirculated through a column of a molecular sieves. This and a tray of P_4O_{10} typically reduced the water content to 1–4 vol ppm. In the later stages of this investigation the N_2 was also recirculated through a column of Ridox (Fisher Scientific) to scavenge the oxygen. The materials are also very reactive with many conventional container materials at elevated temperatures, and so containers of welded niobium tubing[24] (0.95 cm × 7.5 cm) were used, these being also enclosed in evacuated and sealed fused-silica jackets to protect them from the air. Chromel–alumel thermocouples attached to the outside of the jacket opposite the center portion of the Nb tubes monitored the temperatures.

The YCl_3 was prepared from metal and high purity HCl and sublimed in high vacuum.[24] Powdered yttrium was obtained by thermal decomposition of ground (<150 μm) YH_{2-x} in high vacuum ($\lesssim 10^{-5}$ torr), slowly heating the sample to 750 °C until the pressure dropped below discharge. M^ICl compounds, M^I = Li–Cs (Fisher Scientific or J. T. Baker Chemical Co.), were slowly heated in a high vacuum until they sublimed. The Y_2O_3 was obtained within the Ames Laboratory and is the oxide used in the preparation of high-purity metal. YOCl was prepared by heating $YCl_3 \cdot 6H_2O$ to 500–600 °C in a stream of oxygen or air; the product has the PbFCl structure.[25,26]

Compounds of the type M^I_xYClO, M^I = Li–Cs, were first obtained from "ternary" reactions of powdered Y, YCl_3, and M^ICl at >875 °C for 2–4 weeks as irregularly shaped, black plate crystals that grew from the $MCl–YCl_3$ melt systems in 5–60% yields. These were subsequently identified as complex oxides arising from adventitious impurities. This was established first by approximate identification of the extra atom by single-crystal X-ray diffraction studies and then through the preparation of the same phases in high yields by using Y_2O_3 or YOCl as oxygen sources, the correspondence being established by detailed examinations of the Guinier powder patterns.

Reactions of the stoichiometry $xMCl + xY + ((1-x)/3)YCl_3 + ((1-x)/3)Y_2O_3$ were investigated for M = Li–Cs and for $0.09 < x < 0.75$, although not over that range for all M. The equivalent amount of YOCl was also substituted in some instances. The reactions require temperatures above 875 °C, and 2–3 weeks are necessary at 925–950 °C when the system is close to stoichiometry and excess MCl, M_3YCl_6, etc. do not function as a flux. Three different structures are observed for the products. Yields are nearly 100% for two of these within the range $0.14 < x \lesssim 0.25$, with Y and MCl or M_3YCl_6 (and in one case Y_2O_3) also observed for higher x and YOCl for lower x. Intercalates with only the 2H structure were obtained alone in "ternary" reactions, but they were usually admixed with other types in direct oxide reaction.

The above stoichiometry would give a single product phase of composition M_xYClO_{1-x}; however, there is no good evidence that the oxygen coefficient deviates substantially from unity (see Results). Either sufficient traces of oxygen impurities are evidently available, or the reaction is oxygen-limited and small amount of reactants remain. The value of the alkali-metal coefficient x was variable for at least the 3R phase, however, and therefore dependent on the reactant ratios.

Deintercalation Reactions. The deintercalation of K_xYClO was accomplished by vacuum distillation of CH_3CN and I_2 into a reaction flask that contained a 50–60-mg sample. After 1–2 days at room temperature the solvent and excess I_2 were removed by vacuum distillation and powder patterns prepared.

Characterization. The Guinier powder pattern technique was extensively used for phase identification and lattice constant determination. The sample-mounting and data-treatment methods have been described before.[3,27] For calibration, a quadratic function in film position was fitted to the 2θ values of an internal Si standard. Standard least-squares methods were used to calculate lattice constants from 2θ values of indexed patterns. Regular intensity deviations owing to preferred orientation is a common effect with platelike crystals.

Electron microprobe studies using an ARL Model "EMX" instrument with a focused 20-kV beam and a specimen current of 2 nA were conducted on several samples from the "ternary" reactions. The transfer of the sample to the spectrometer was accomplished in a N_2-filled glovebag attached to the port of the spectrometer. The results from reactions with M^I = K and Cs yielded average compositions of $3R\text{-}K_{0.17}YCl_{1.02}$ (Y_2O_3 reaction, $x = 0.33$), $2H\text{-}K_{0.12}YCl_{0.98}$ (ternary reaction) and $2H\text{-}Cs_{0.10}YCl_{0.99}$ (ternary) when normalized to yttrium; oxygen was not determinable. There was no significant deviation of the Y:Cl ratio from unity, indicating that the surfaces of the crystals were virtually salt-free.

Table I. Diffraction and Refinement Data

	$2H\text{-}K_{0.08}YClO$	$3R\text{-}Na_{0.08}YClO$
cryst size, mm	0.3 × 0.3 × 0.01	0.3 × 0.3 × 0.01
space group	$P6_3/mmc$	$R\bar{3}m$
cell, dimens, Å		
a	3.7873 (6)	3.7881 (3)
c	21.860 (8)	29.445 (5)
octants measd	4	4
2θ(max), deg	50	50
reflcn data		
checked	1336	1794
obsd ($>3\sigma(I)$)	934	501
indep reflcns	141	101
R(av)	0.065	0.074
structure solution[a]		
R	0.057	0.109
R_w	0.075	0.122
no. of variables	12	11

[a] $R = \sum||F_o| - |F_c||/\sum|F_o|$; $R_w = [(\sum w(|F_o| - |F_c|)^2/\sum w|F_o|^2]^{1/2}$.

Suitable single crystals in the form of thin plates were mounted in 0.3 mm i.d., thin-walled capillaries in a drybox under 15-power magnification. Oscillation and zero- and first-level Weissenberg photographs were used to establish their singularity, diffracting ability, and quality as well as their symmetry and the absence of any intergrowth or superstructure.

All single-crystal data sets were collected with monochromatic Mo Kα radiation (λ = 0.710 34 Å) on the Ames Laboratory four-circle diffractometer with the customary standard reflections; no evidence of decay was noted. Details regarding the data collection and structure solution are summarized in Table I. The absorption coefficient of yttrium for Mo radiation is particularly large since it lies on the absorption edge, so both data sets were corrected for absorption by using a ψ-scan method with the reflection tuned every 10° in φ and the program ABSN.[28] Four octants of data were collected with no restrictions in both cases. Averaging the observed reflections yielded the independent data sets with no reflections eliminated by a cutoff of 6σ from the average. Final lattice dimensions were obtained by a least-squares fit of 14 reflections ($25° < 2\theta < 40°$), each of which was tuned on both Friedel-related peaks. Structure factor calculations and full-matrix least-squares refinements were carried out with the program ALLS[29] while Fourier series calculations were done with FOUR.[30]

Structure Solutions. The refinement of the structure of $2H\text{-}K_{0.08}YClO_{0.82}$ was carried out in the space group $P6_3/mmc$ on the basis of Weissenberg photographs that showed the $00l$, $l = 2n + 1$, and $h - k = 3n$, $l = 2n + 1$, extinction conditions were present. Examination of the diffractometer data showed there were 43 violations of the second extinction condition for which F_o ranged from 7 to 71. Closer examination of these reflections showed that all were spurious; most were not observed every time, there was always an overlap with strong adjacent peaks, and the observed "peak" profiles had no maxima. The data set was absorption corrected and reduced with the extinction conditions applied.

The structure was solved by using a Patterson map, which indicated the yttrium positions. An apparent solution of the structure was obtained with an $R = 0.14$ and a composition of $K_{0.06}YCl$. At first, it was believed that this was the correct solution of the structure and that the extra peak in the electron density and difference maps and the large R value were the result of poor crystal quality. However, the long Y–Y interlayer distances, 3.57 Å in the supposedly more reduced phase vs. 3.511 Å in YCl, could not be explained, and this led to reassessment of the structure. Closer examination revealed that the extra peak was in the tetrahedral-like interstice between the yttrium layers. This position and distances of approximately 2.25 Å to yttrium were all reasonable for an oxygen atom. Insertion of an oxygen atom and variation of the position dropped the R to 0.062. The structure refined well to a final $R = 0.057$ and $R_w = 0.075$ on varying the positions and anisotropic thermal parameters on Y and Cl and the multipliers and isotropic B's on K and O. Subsequent direct synthesis of the phase in high yield established the correctness of the interstitial assignment.

A second data set was collected on a black plate crystal obtained from a "ternary" $NaCl/YCl_3/Y$ reaction, $Na_{0.08}YClO_{1.0}$. Weissenberg photographs and the crystal data showed that the R-centering extinction

(24) Corbett, J. D. *Inorg. Synth.* **1983**, *22*, 15, 39.
(25) "Gmelins Handbuch der Anorganischen Chemie", 8th ed.; Springer-Verlag: West Berlin, 1974; Vol. 39, Part C5, p 17.
(26) Hulliger, F. "Structural Chemistry of Layer-Type Phases"; Lévy, F., Ed.; D. Reidel Publishing Co.: Boston, MA, 1976.
(27) Cisar, A. J.; Corbett, J. D.; Daake, R. L. *Inorg. Chem.* **1979**, *18*, 336.
(28) Karcher, B. Ph.D. Dissertation, Iowa State University, Ames, IA, 1981.
(29) Lapp, R. L.; Jacobson, R. A. DOE Report IS-4708; Ames Laboratory: Iowa State University, Ames, IA, 1979.
(30) Powell, D. R.; Jacobson, R. A. DOE Report IS-4737; Ames Laboratory: Iowa State University, Ames, IA, 1980.

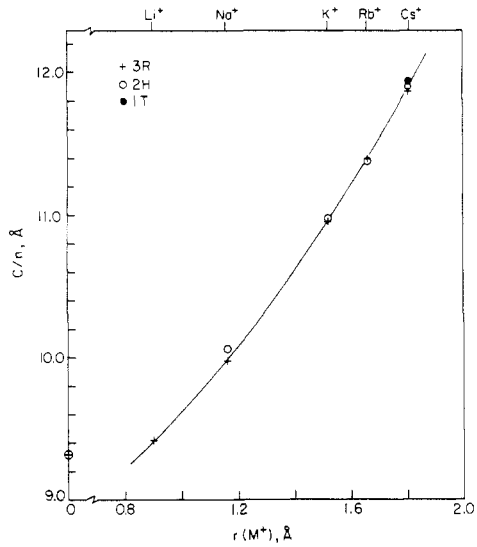

Figure 1. The *c*-axis length per slab (c/n, Å) in M^I_xYClO as a function of M^I cation radius: (+) 3R; (○) 2H; (●) 1T; (⊕) 3R-YClO.

condition was present, $-h + k + l \neq 3n$, and the lattice dimensions were also consistent with an expanded YCl-type structure. The data were absorption corrected, reduced with the *R*-centering condition applied, and averaged in $R\bar{3}m$. Trial yttrium and chlorine positions were taken from the YCl structure, and isotropic refinement of these resulted in $R = 0.215$ and $R_w = 0.258$. The oxygen and sodium positions were determined from the resulting electron density map. Varying the positions and anisotropic thermal parameters on Y and Cl and the position, multiplier, and isotropic *B* on oxygen yielded $R = 0.112$ and $R_w = 0.125$. The multiplier and *B* for sodium could not be varied simultaneously. These were instead alternately varied on successive cycles, and the structure was refined to $R = 0.109$ and $R_w = 0.122$.

The difference electron density map showed an extra peak at 0,0,0.454 of ~2.3 electrons. The extra peak is not in any type of an interstitial position in the structure but is slightly displaced from the metal layers toward the oxygen layers. The distances from the extra peak to neighboring atoms are very unreasonable for any bonding, e.g. at 1.83, 2.19, and 2.21 Å from Cl, Y, and O, respectively. This implies the peak is not the result of an atom. The extra peak and the limited quality of the refinement were probably caused by poor crystal quality, which was evident in the averaging of the data and in the Weissenberg photos that showed streaking along all festoons. The streaking along the festoons was also observed for the 2H phase, but in this case the streaks had only 10% of the intensity of the large peaks. The streaking implies some degree of disorder along c^*.

Results

Briefly, the reactions of appropriate proportions of M^ICl, Y, YCl_3, and Y_2O_3 for 2–3 weeks above 900 °C give high yields of intercalated YOCl products M^I_xYClO in three structural series, 3R (Li–Cs), 2H (Na-Cs), and 1T type (Cs). The host structure in all of these consists of slabs with close-packed layers sequenced Cl–Y–O–O–Y–Cl. The alkali-metal coefficient *x* in the first and the last types and the product distribution for a given M^I depend on reaction stoichiometry. The 2H type is not found when preformed YOCl rather than YCl_3 and Y_2O_3 is the reactant, evidently because YOCl (PbFCl type) can undergo a topotactic conversion via a YOF-type intermediate only to the 3R or 1T structures. The structural details of the 3R- and 2H-type series are known through single-crystal diffraction studies. The 3R type of M^I_xYClO is converted to crystalline YOCl in a YOF-type structure by I_2, and most 3R- and 2H-type phases can be coherently and reversibly hydrated by water vapor to 1T- and 2H-type structures, respectively. Each of these aspects will now be considered separately in more detail.

Synthesis and Stoichiometry. Compounds of the general formula type M^I_xYClO, M^I = Li–Cs, were first obtained accidentally via impurities present during reactions of powdered Y, YCl_3, and M^ICl at temperatures greater than 875 °C for 2–4 weeks. These products occurred as irregularly shaped black plate crystals, which grew from the melt in yields of 5–60%. All powder patterns could be indexed with a hexagonal cell with *a* slightly larger than in YCl[6] and a *c*-axis value corresponding approximately to the insertion of alkali metal in every Cl–Cl gap (stage one) of a two-slab structure type. The regularities in dimensions that were eventually sorted out are shown in Figure 1, the thickness per slab, c/n where *n* is the number of slabs per cell, vs. M^I crystal radii[31] for the three types of M^I_xYClO phases. At first it was assumed that these compounds were the ternary M^I_xYCl phases. It was not until the crystal structure of 2H-$K_{0.08}YClO_{0.82}$ was solved (below) that the character of these compounds was discovered, that something was bound in the tetrahedral-like interstices between the yttrium layers. The presence of a second series was forecasted by a structural study of 3R-$Na_{0.08}YClO$. Subsequent reactions using Y_2O_3 or YOCl as oxygen sources gave high yields of the same phases that had been generated in the "ternary" reactions by what must have been oxygen impurities. The most likely source of the oxygen in the early work was a contaminated batch of powdered yttrium, but other possibilities were the YCl_3 and M^ICl salts, degassing of the silica jacket, and unremoved cleaning solution from the crimped end of the metal container that was welded before loading. The presence of oxygen was also confirmed qualitatively by microprobe in a sample of 3R-$K_{0.17}YCl_{1.02}O_y$.

The best route to these phases is the direct reaction of MCl, Y, YCl_3, and Y_2O_3 (or YOCl) at 925–975 °C for a few weeks. Most of the reactions were studied for the stoichiometry

$$x\mathrm{MCl} + x\mathrm{Y} + ((1-x)/3)\mathrm{YCl_3} + ((1-x)/3)\mathrm{Y_2O_3} \rightarrow \mathrm{M}_x\mathrm{YClO}_{1-x} \quad (1)$$

or, with preformed YOCl

$$x\mathrm{MCl} + x\mathrm{Y} + (1-x)\mathrm{YOCl} \rightarrow \mathrm{M}_x\mathrm{YClO}_{1-x} \quad (2)$$

Two structural types are generally found for the product, namely the 2H type (M = Na–Cs) and the 3R type (M = Li–Cs), and the polytype distribution from reaction 1 depends on the value of *x* used as does the alkali-metal content of the nonstoichiometric 3R phase, as written, the 3R-type product increasing with the amount of MCl used. A third structure is also found for cesium, 1T-Cs_xYClO. The use of YOCl in reaction 2 rather than Y_2O_3 and YCl_3 provides *only* 3R-M_xYClO (plus 1T-Cs_xYClO). On the other hand, only the 2H-M_xYClO phase was obtained (plus the analogous carbides[17] sometimes) from the oxygen-limited "ternary" MCl/Y/YCl_3 reactions (except for M = Li where only 3R is stable) unless the relative amount of MCl was quite high. There is no good evidence that the products are significantly oxygen deficient relative to M_xYClO, in which case the above reactions will be slightly incomplete if the amount of adventitious oxygen is not comparable to *x*.

The total yields of the M_xYClO phases are nearly 100% in the range $0.14 < x \lesssim 0.25$ (reaction 1), with YOCl remaining for lower values. Table II summarizes the compounds obtained, typical lattice constants, and some of the pertinent conditions. In the K_xYClO system, there was a 100% yield of K_xYClO for $x \sim 0.17$, namely 60–70% of the 2H form with the remainder being the 3R type. Lower *x* values gave mainly the 2 H form while for $x > 0.20$ only 3R-K_xYClO (and some Y_2O_3) was obtained. Although a straightforward interpretation of this would be that the 2H form is poorer in M (and possibly in oxygen), the distribution of 3R and 2H types may in fact depend on the character of an accompanying Y_2O_3/YCl_3 reaction that forms YOCl. This will be more apprent when type 2 reactions are considered. Other systems, M^I = Na, Rb, and Cs, show similar trends but were not studied as extensively. The sodium system gave only the 2H structure at $x = 0.17$ and 2H- and 3R-type mixtures at $x = 0.32$–0.51. A single product, 2H-Na_xYClO, was obtained for $x = 0.19$ and 10% excess YCl_3. No intercalated product was found with $CaCl_2$.

Reaction 2 using YOCl has the advantage of yielding only the 3R form (plus 1T-Cs), and so this has been studied at some length for M^I = K. After 2–3 weeks at 945 °C, reactions with $x = 0.35$

(31) Shannon, R. D. *Acta Crystallogr., Sec. A: Cryst. Phys., Diffr., Theor. Gen. Crystallogr.* **1976**, *A32*, 751.

Table II. Guinier Lattice Constants (Å) of M^I_xYClO, YClO, and $M^I_x(H_2O)_aYClO$ Phases

	a	*c*	*a*(max)	*c*(max)	$\Delta(c/n)^e$
		3R-$M^I_xYClO^a$			
Li	3.7873 (1)	28.197 (4)	3.7872 (2)	28.262 (5)	
Na	3.7883 (5)	29.947 (8)			
K	3.7894 (2)	32.76 (1)	3.7908 (3)	32.881 (9)	
Rb	3.7890 (4)	34.13 (1)			
Cs	3.7933 (4)	35.47 (2)	3.7939 (5)	35.58 (2)	
		2H-$M^I_xYClO^a$			
Na	3.7863 (5)	20.13 (1)			
K	3.7894 (2)	21.939 (4)			
Rb	3.7888 (3)	22.737 (6)			
Cs[b]	3.7920 (2)	23.818 (3)			
		1T-M^I_xYClO			
Cs	3.7919 (2)	11.932 (9)[b]	3.7915 (4)	12.06 (1)	
		Deintercalate[c]			
3R-YClO	3.7968 (3)	27.960 (8)			
		Hydrates[d]			
3R-K[f]	3.7910 (2)	32.887 (8)			
1T-K hydrate	3.7857 (4)	11.864 (5)			2.54
3R-K dehydrate	3.7900 (6)	32.87 (1)			
3R-Rb	3.7909 (4)	34.10 (1)			
1T-Rb hydrate	3.7873 (4)	11.88 (1)			2.56
2H-Rb	3.7888 (3)	22.737 (6)			
2H-Rb hydrate	3.7881 (2)	23.834 (7)			2.60

[a] Mean values for reactions near $x = 0.18$; maximum values for reaction 2 with $x \geq 0.25$. [b] Reaction 1 with $x = 0.14$. [c] From 3R-K_xYClO. [d] M^I_xYClO hydrated by exposure to moist air. [e] The *c*-axis length per slab relative to that in 3R-YClO. [f] Anhydrous starting material.

and 0.30 yielded 3R-K_xYClO and unreacted KCl and Y. For $x = 0.25$, 0.18, and 0.15 there was a nearly quantitative yield of the 3R-phase. A 70% yield of 3R type together with YOCl was obtained for $x = 0.11$. Y_2O_3 was also found in this system for $x \geq 0.25$, but not for Li or Na ($x \leq 0.75$) or Rb or Cs ($x \leq 0.3$). The implication is that other equilibria are important, namely the disproportionation of K_xYClO or YOCl (to K_3YCl_6 etc.) with higher KCl concentrations, also signaling that the system is not oxygen deficient. Such a YOCl decomposition in KCl melts has been seen in another context.[23]

The lattice constants and alkali-metal content of the 3R phases clearly depend on reactant stoichiometry. The dependence of the *c* axis of 3R-K_xYClO on *x*, the number of moles of KCl in reaction 2, is presented in Figure 2. The number of data points is limited but the data clearly show that the axis length increases with the concentration of KCl until the stoichiometric *x* reaches ~0.27. The *x* plotted here equals the potassium coefficient only over the one-phase region, but the latter (and the lattic constant) clearly continues to increase (or decrease) outside of this region with changes in KCl (*x*) when Y_2O_3 (or YOCl) are also present. No useful information was gained from a plot of the *a*-axis length vs. composition. The upper limit is similar for 3R-Li_xYClO based on the appearance of LiCl (and Y) between a stoichiometric *x* of 0.25 and 0.27.

It should be noted that, in contrast to the behavior of all other phases, the Guinier powder patterns of the 2H-Na_xYClO phase produced in both "ternary" and quaternary reactions show significant broadening of many lines. This naturally leads to larger standard deviations of the lattice parameters. Weissenberg photographs of 2H-Na_xYClO (0 to 4th level in *k*) show streaking along all festoons where $h - k \neq 3n$ while all festoons with $h - k = 3n$ contain only single spots. These effects correlate with the broad lines in the powder patterns by the same $h - k \neq 3n$ condition. These observations are characteristic of random stacking faults perpendicular to the layers[32] and may well be related to the cause of the relatively large *c* lattice constant found for sodium (Figure 1), the smallest cation that forms this structure

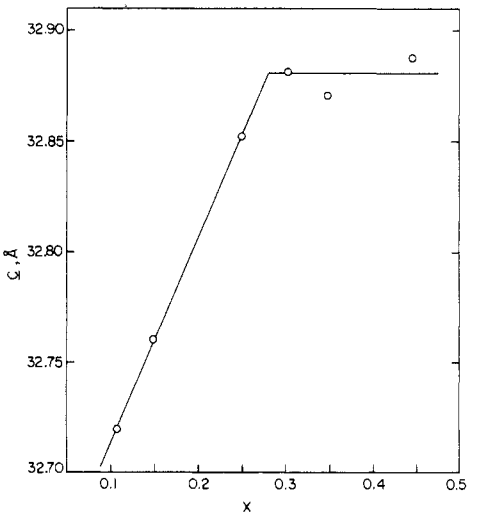

Figure 2. Dependence of the *c* lattice constant of 3R-K_xYClO on stoichiometry *x* from the reaction xKCl + xY + $(1 - x)$YOCl.

type. On the other hand, powder patterns of 3R-Na_xYClO contain only sharp lines and are in very good agreement with those calculated on the basis of the 3R-$Na_{0.08}YClO$ structure (below).

Reactions in the cesium system were somewhat different. Irregular foil-like crystals of 1T-Cs_xYClO up to 1 to 2 cm across were found in "ternary" systems, and this phase was also formed in more conventional reactions with Y_2O_3. The latter were virtually quantitative at $x = 0.14$ to give a roughly 5:3:2 mixture of the 1T, 2H, and 3R forms. The 2H type disappeared at $x = 0.18$, as observed in other systems. Type 2 reactions with YOCl gave nearly quantitative yields over the range $0.14 \leq x \leq 0.29$, with approximately equal amounts of 1T and 3R types at $x \sim 0.24$ and, surprisingly, only 1T-Cs_xYClO at both extremes. However, annealing the mixture above 900 °C for ~4 days has been observed to convert 3R to the 1T type. The reaction time is thus also a variable, and the reaction at higher *x* that gave only the 1T form was cooled slowly. The *c* lattice constant of 1T-Cs_xYClO was observed to increase 1.5% over the indicated range, considerably greater than the change seen in Figure 2, implying

(32) Trigunayat, G. C.; Verma, A. R. In "Crystallography and Crystal Chemistry of Materials with Layered Structures"; Lévy, F., Ed.; D. Reidel: Boston, 1976; p 318.

Table III. Positional, Thermal, and Lattice Parameters for YCl,[a] 3R-$Na_{0.08}YClO$, and 2H-$K_{0.08}YClO$

	z				occupancy	
	Y	Cl	O	M^I	M^I	O
YCl[b,c]	0.21683 (5)	0.3883 (1)				
3R-$Na_{0.08(3)}YClO_{1.0(1)}$[b,c]	0.2148 (1)	0.3915 (3)	0.1306 (8)	0	0.08 (3)	1.0 (1)
2H-$K_{0.08(6)}YClO_{0.82(6)}$[d]	0.06447 (9)[e]	0.1469 (3)[e]	0.0400 (17)[f]	$^1/_4$[f]	0.08 (2)	0.82 (6)

	B_{11}[g]		B_{33}		B		lattice const,[h] Å	
	Y	Cl	Y	Cl	M^I	O	*a*	*c*
YCl	1.08 (6)	1.5 (1)	1.31 (9)	1.2 (1)			3.7523 (2)	27.525 (5)
3R-$Na_{0.08(3)}YClO_{1.0(1)}$	0.53 (15)	1.3 (3)	2.9 (2)	1.6 (4)	1.25	0.7 (8)	3.7881 (3)	29.445 (5)
2H-$K_{0.08(6)}YClO_{0.82(6)}$	1.16 (9)	1.6 (2)	2.7 (1)	2.8 (2)	0.8 (5)	3.0 (16)	3.7873 (6)	21.860 (8)

[a] Reference 6. [b] $R\bar{3}m$ space group. [c] $x = y = 0$. [d] $P6_3/mmc$ space group. [e] $x = {}^1/_3, y = {}^2/_3$. [f] $x = {}^2/_3, y = {}^1/_3$. [g] $\exp[{}^1/_4(B_{11}a^{*2}(h^2 + hk + k^2) + B_{33}l^2c^{*2})]$. [h] Diffractometer data.

Table IV. Comparative Distances (Å) in YCl, 3R-$Na_{0.08}YClO$, and 2H-$K_{0.08}YClO$

	YCl	2H-$K_{0.08}YClO$	3R-$Na_{0.08}YClO$
		Intralayer	
Y–Y, Cl–Cl, O–O (6×)	3.7523 (2)	3.7873 (6)	3.7881 (3)
		Interlayer	
Y–Y (3×)	3.511 (2)	3.567 (3)	3.581 (7)
Y–Cl (3×)	2.750 (2)	2.833 (4)	2.820 (7)
Y–O (1×)		2.284 (15)	2.472 (25)
Y–O (3×)		2.251 (4)	2.217 (4)
O–O (3×)		2.80 (2)	3.038 (33)
M^I–Cl (6×)		3.140 (4)	2.776 (6)
M^I–Cl(calcd)[a]		3.19	2.83

[a] Crystal radii, CN = 6, from ref 31.

a sizable range of cesium composition.

While slow cooling altered the proportions significantly in favor of the 1T type, it also improved the product crystallinity, but not to the point where crystals of either phase were adequate for single-crystal studies.

Structure Solutions. The final atom parameters for 2H-$K_{0.08}YClO$ and 3R-$Na_{0.08}YClO$ are given in Table III, and bond distances in these and in YCl (or $YClH_y$[14]) are compared in Table IV. The [110] sections of the three are shown in Figure 3.[33]

The basic unit in all intercalate structures is a Cl–Y–O–O–Y–Cl slab consisting of four cubic-closed-packed layers sequenced Cl–Y–Y–Cl with oxygen atoms in the tetrahedral-like interstices between the metal layers. This arrangement is also basic to the structures of YClH, ZrCl (with empty interstices), and $ZrXO_y$. As seen in Figure 3c, the layering geometry in the 2H-type structure for just the chlorine (upper case letters) and yttrium layers is ...|AbcA|AcbA |... or, alternately, in terms of slabs, ...AA′... where the A′ slab involves a reversal of the metal atom positions relative to those in the A slab. The sequence within the two slabs is thus different from that in 3R-M^I_xYClO, ZrBr, YOCl, etc., ...ACB..., meaning that the 2H-type structure cannot be generated from those of the 3R or 1T types, or vice versa, by only interslab slippage; rather, a reconstruction of every other slab is required. This factor is important to the specificity of synthesis reaction 2 starting with YOCl and will be returned to in the Discussion section.

The placement of all chlorine atoms in 0,0,*z* positions in the 2H phase results in trigonal-prismatic holes for alkali metal between the chlorine layers. There are two possible sets of trigonal-prismatic holes, and potassium reasonably occupies the one with oxygen atoms as second nearest neighbors. The refined occupancy of potassium, 0.08 (±0.06), and the absence of any evidence for a superstructure indicates the metal is randomly distributed over roughly 16% of the sites.

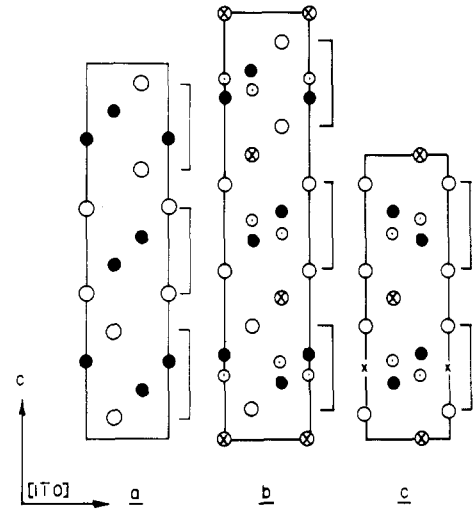

Figure 3. [110] sections of the unit cells of (a) 3R-YCl, (b) 3R-M^I_xY-ClO, and (c) 2H-M^I_xYClO with brackets marking the slabs (× is the correct origin in c): (○) Cl; (●) Y; (⊙) O; (⊗) M^I.

The advantage of potassium having two oxygen atoms as second nearest neighbors may be responsible for the trigonal-prismatic coordination around potassium rather than an antiprismatic arrangement that could be easily obtained with the sequence (AbcA)(BacB) (space group $P6_3mc$). In any case, powder patterns calculated on the basis of the refined 2H-structure parameters agree very well with those of all the observed 2H-type phases while those calculated for this alternate packing are distinctly inferior.

The structure of 3R-M^I_xYClO retains the basic ordering of YCl (Figure 3) as described by the layering geometry ...|AbcA|-CabC|BcaB |... or ...ACB... with all the tetrahedral-like interstices between the yttrium layers filled with oxygen and the expanded trigonal-antiprismatic holes between the chlorine layers randomly occupied with alkali metal. The compounds are isostructural with $ZrBrO_x$[15] and YOF,[34] ignoring the alkali metal atoms. The crystal studied came from a reaction of adventitious oxygen with a NaCl-rich melt with YCl_3 and excess metal. Clearly higher alkali-metal contents can be obtained in direct reactions (Figure 2 and Table II). The appreciable asymmetry of the thermal ellipsoids observed for yttrium but not chlorine *may* result from charge localization at this low level of reduction. Suitable single crystals were not obtained from the high-yield, direct reactions, crystal growth being much favored by the excess MCl–YCl_3 melts.

The distances in the two structures are all very reasonable. As seen in Table IV, the inter- and intralayer Y–Y distances increase slightly relative to those of YCl (or $YClH_y$[14]) to accommodate the oxygen in the tetrahedral-like interstices. The average Y–O distances of 2.26 and 2.28 Å are very reasonable when compared

(33) Hexagonal nets that are close-packed in any sequence are conventionally given A, B, and C representations of their relative orientation in projection. This description also may be applied to interstitial atoms in tetrahedral, octahedral, or trigonal prismatic orientation between the layers. The [110] sections of such structures are very convenient pictorials since all atoms lie on such planes.

(34) Mann, A. W.; Beven, D. J. M. *Acta Crystallogr., Sect. B: Struct. Crystallogr. Cryst. Chem.* **1970**, *B26*, 2129.

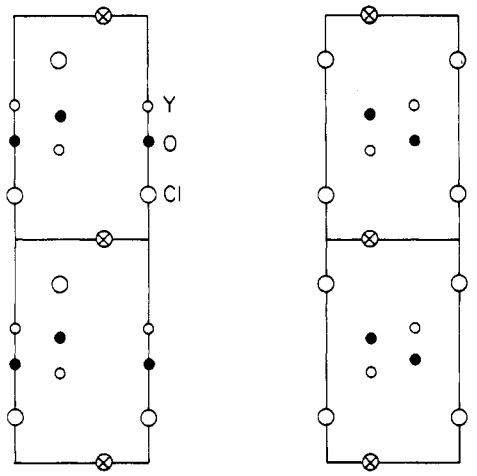

Figure 4. Alternative structures for 1T-M_xYClO (double cells). Left—hcp; right—ccp (1T-Cs_xYClO): (○) Cl; (●) Y; (○) O; (⊗) M.

with Y–O distances of 2.28 Å in Y_2O_3[35] and 2.27 Å in both YOCl (PbFCl structure type)[26] and YOF.[34] Actually, there is a fair asymmetry in the Y–O distances in 3R-$Na_{0.08}YClO$, apparently because of a poorly conditioned refinement. An electron density map indicated the oxygen was in the center (±0.02 Å) of the tetrahedral-like interstice, but the atom moved toward the basal yttrium atoms during least-squares refinement. This type of behavior has also been observed in $ZrBrO_{0.29}$.[15] The M^I–Cl distances are each about 0.05 Å less than the sum of crystal radii, perhaps because of both the covalent bonding of chlorine to yttrium and the low (~16%) occupancy of the M^I sites (Figure 2).

The precise oxygen contents of these phases are not well established, and all formulas have simply assumed 1:1:1 for Y:Cl:O. The refined coefficients in the single-crystal studies, 0.83 (6) for the 2H phase and 1.0 (1) in the 3R example, are perhaps not distinguishable from unity. However, the 2H phase did form preferentially in the "ternary" MCl–YCl_3–Y systems at low oxygen levels. In addition, the *c* lattice constants for 2H phases were somewhat lower when isolated from oxygen-poor "ternary" systems. This was especially so for 3R-Na_xYClO (compare Tables II and III) as well, although the 3R systems also appear to be significantly nonstoichiometric in alkali-metal content.

The probable structure of 1T-Cs_xYClO was established by a comparison with powder patterns calculated on the basis of reasonable models. Only two seem possible for this simple a cell, yttrium and chlorine layers stacked in either the hcp AbaB or the ccp AbcA, both presumably with oxygen in the tetrahedral-like interstices between yttrium layers. These alternatives are shown in Figure 4. The first, with the sequence Ab(a)(b)aB (oxygen in parentheses), is considered improbable both because of the close approach of chlorine and oxygen along *c*, an exclusion that appears fairly general among interstitial derivatives, and because of its lack of a ready interconvertability with the 3R structure important both in its formation and with the structurally very similar hydrate (vide infra). The second, ccp arrangement avoids both of these problems and gives calculated intensities that are in good agreement with observation. There are two equivalent trigonal-prismatic sites for cesium between the chlorine layers that cannot be distinguished by the powder data, and disorder over both may in fact be involved. The cesium sites would have one oxygen and one yttrium as second nearest neighbors out at the ends of the chlorine trigonal prism, which is somewhat unusual.

Powder patterns of only 1T-Cs_xYClO show two weak lines (10–20% of the strongest) that cannot be accounted for by known phases, and sometimes one or two others are also seen in powder patterns of mixtures. All extra lines can be indexed with a supercell, best done by tripling *a* and *b*. This suggests the cesium atoms order in a more complex way in the trigonal-prismatic sites.

Table V. Lattice Constants (Å) of 3R-YClO from Oxidation of 3R-M^I_xYClO by I_2 (CH_3CN, 22 °C)

M^I	time, days	3R-YClO *a*	3R-YClO *c*	M_xYClO *c*
K (2H + 3R)	3	3.7950 (2)	27.938 (8)	32.893 (7)
K	2	3.7968 (3)	27.960 (8)	32.887 (8)
Li	3	3.7899 (3)	28.021 (6)	28.259 (4)
lit.[a]		3.7895 (5)	28.03 (1)	
		3.781 (2)	27.93 (1)	

[a] From Y_2O_3–NH_4Cl–H_2O reactions.[23]

Deintercalation. Since one definition of intercalation requires that it be reversible, it was desirable to show that the alkali metals in M_xYClO could be removed. The oxidation of 2H- and 3R-M^I_xYClO to YClO was accomplished with I_2 and M^I = Li, K according to (3). The lattice constants obtained after the reaction are included in Table V.

$$M^I_xYClO + (x/2)I_2 \text{ (in } CH_3CN) \rightarrow YClO + xM^II \quad (3)$$

The powder patterns of the black powder and chunks obtained after the 3R reaction showed sharp lines that could be indexed as a 3R-type structure. A particularly striking feature of the process was the shift of the 003 line of 3R-K_xYClO from 11.476 to 9.342 Å. A calculated powder pattern for the latter based on the structures of YOF[34] or the isostructural $ZrBrO_x$[15] was in excellent agreement with observation. Thus oxidation of the 3R intercalate at room temperature leads to a coherent conversion to alkali-metal-free YClO in a new structure. The same 3R-YClO phase (as well as those for Ho, Er, and Tm) has subsequently been obtained by a low-temperature pyrohydrolysis of $(NH_4)_3YCl_6$.[23] The close correspondence between powder patterns and the lattice constants (Table V) clearly indicates the two routes give the same product.

A K_xYClO sample that initially contained both the 2H and 3R phases gave sharp diffraction lines from 3R-YClO and very broad lines from the 2H form after reaction 3. A calculated powder pattern for 2H-YClO, based on the collapsed 2H-$K_{0.08}YClO$ structure, matched the positions of the broad lines. However, removal of the alkali metal from the M^I-2H structure results in a non-close-packed arrangement of slabs, and the disorder caused by the movement of the slabs toward close-packed arrangements produces the broad lines.

The products of the oxidative deintercalation are still dark colored, suggesting either incomplete reaction or reduced species within the slabs. This probably means only that no diffusion reactions occur within the slabs at room temperature. The oxychlorides of most rare-earth-metal elements are dark colored to black after being equilibrated with metal at high temperature; LaClO (PbFCl type) for example, is black but with no significant difference in lattice constants from those of the normally white material.

Reintercalation of the above 3R-YClO with 1.6–2.4 M solutions of C_4H_9Li in hexane at room temperature or 60 °C was unsuccessful. In addition, 3R-YClO dispersed in alkaline solutions (pH 8–10) of sodium dithionite showed no reaction. A relatively strong reducing agent would be expected to be necessary to react with yttrium(III), and sodium in liquid NH_3 has proven to be effective.[23]

Hydration. The different powder patterns obtained after 3R-K_xYClO samples had been exposed to air for 1 h to 8 d could be indexed well as an expanded, one-slab structure. The best explanation for this change is that the sample had been hydrated with very little or no oxidation. A sample of the new phase heated under vacuum at 270 °C for 1 h gave a weight loss of 2.3 (5)%, which corresponds very well to $K_x(H_2O)_aYClO$ with $a \simeq x$ and an estimated *x* value of 0.20. Such a 1:1 ratio for K:H_2O is similar to the extent of the hydration of $M^I_xMS_2$ compounds reported by Röder et al.[36]

(35) O'Connor, B. H.; Valentine, T. M. *Acta Crystallogr., Sect. B: Struct. Crystallogr. Cryst. Chem.* **1969**, *B25*, 2140.

(36) Röder, U.; Müller-Warmuth, W.; Schöllhorn, R. *J. Chem. Phys.* **1979**, *70*, 2864.

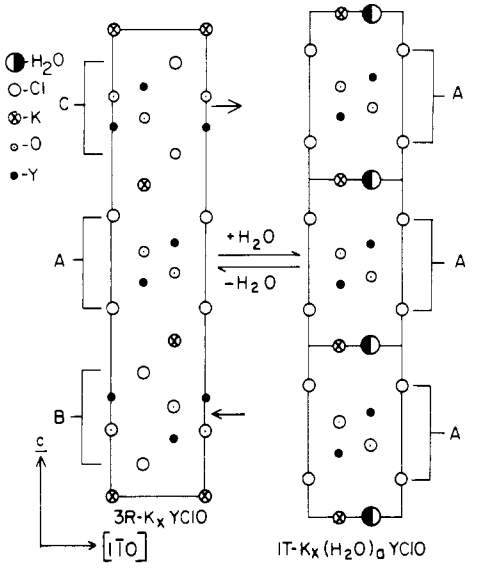

Figure 5. Proposed slab-sliding process for the conversion of 3R-K_xYClO to 1T-$K_x(H_2O)_aYClO$.

A remarkable result of this hydration and dehydration sequence is that the powder pattern of the final product is the same as that of the original 3R-K_xYClO phase, with no discernible line broadening. Lattice constants of the original 3R-K_xYClO, the hydrate 1T-$K_x(H_2O)_aYClO$, and 3R-K_xYClO after dehydration were given in Table II, where it will be seen that the 3R-K_xYClO lattice parameters before and after differ by less than 1σ. Such good retention of order during the 3R $\rightleftarrows$ 1T conversion in spite of a 2.5-Å change in slab separation suggests that hydrogen bonding between the outer chlorine layers in the slabs plays an important role in the process.

Similar hydrates of both 2H- and 3R-Rb_xYClO have also been observed (Table II). The 3R-type phase formed a one-slab hydrate, analogous to potassium. When the 2H phase was hydrated in air, the powder pattern simply shifted to lower 2θ values and could be indexed as an expanded two-slab structure. Since there were no changes in intensities and no extra lines appeared, it is assumed that the same structure applies for 2H-$Rb_x(H_2O)_aYClO$ (space group $P6_3/mmc$), with the water accommodated in the empty set of trigonal-prismatic holes, analogous to the 1T structure (below).

Ground samples of 3R-Li_xYClO left in air for several days showed no evidence of hydration. It should be noted that all hydration studies were carried out during the winter months, i.e., at relatively low humidities ($\lesssim$30–35%). The Na_xYClO and Cs_xYClO phases were not examined for hydration products.

A structural model for 1T-$M^I_x(H_2O)_aYClO$ was obtained by considering the two possible arrangements for a one-slab structure, the same procedure as described above for the isostructural but anhydrous 1T-Cs_xYClO. The model necessarily retains the 3R-type slabs, each with a ccp arrangement AbcA and oxygen in the tetrahedral interstices, and provides trigonal-prismatic coordination for M^I. In this case there were no extra lines suggestive of a superlattice, and calculated powder patterns based on the ccp-packed slabs matched the observed powder patterns for the hydrates very well. The observed and calculated powder patterns for the potassium hydrate and for 1T-Cs_xYClO are given in the supplemental material. With fractional occupancy of M^I it is possible that the alkali metal and water molecules are disordered over the two adjacent trigonal-prismatic sites. The reversible 3R $\rightleftarrows$ 1T change on hydration can be easily achieved by a "sliding" of the individual slabs, as shown in Figure 5, and is presumably guided by hydrogen bonding of water to the adjacent chlorine layers.

The powder patterns and the lattice constants of what are considered to be 1T-$Rb_x(H_2O)_aYClO$ and 1T-Cs_xYClO are virtually identical (Table II), and some consideration was given to the possibility that the latter had accidentally become hydrated, either in the "dry box" or as mounted on tape for the pattern. As unlikely as this seemed, it was established not to be the case by heating a weighed sample of the cesium salts (50:50 1T:3R) to 270 °C in high vacuum. No change in either the weight or the subsequent powder pattern was found. A close similarity in radius between cesium and hydrated rubidium in the intercalate is in itself quite reasonable.

Exfoliation. The effect of liquid water on M^I_xYClO samples was first observed under the microscope with a sample of 3R-K_xYClO. Initially, the chunk broke into small platelike pieces with gas evolution, presumably H_2 from oxidation. The black plates slowly turned brown, and each exfoliated into accordionlike pieces. The increase in the thin-plate direction was generally greater than 100-fold. With time, the "crystals" transformed from a translucent brown to a translucent green. When the exfoliated "crystal" was removed from the water, the heat from the microscope light caused the "crystal" to shrink back down to a thin plate. This process was reversible, although the effect was somewhat diminished with each repetition. The dehydrated plate was usually dark green around the edges and light green or transparent in the middle. The longer the crystals remained in the water the clearer and more translucent they became. Even after four hours in water, the exfoliated "crystals" could be dehydrated to form clear plates. As might be expected, powder patterns of the collapsed plates showed only very broad lines. Heating them to ~110 °C terminates the reversible exfoliation, presumably by removing the last trace of water bound to the chlorine faces of the slabs.

This effect has also been observed with other 3R-M^I_xYClO phases for M^I = Li–Cs. With 3R-Cs_xYClO, the rate of formation of the exfoliated plates was noticeably slower, which may be associated with the smaller hydration energy of Cs^+. Samples of 2H-M^I_xYClO or 3R-YClO did not show any appreciable exfoliation with water.

Discussion

The 1T, 2H, and 3R-M^I_xYClO phases can all be viewed as end members of a series of oxygen interstitial derivatives of the four-layer slabs in the parent YCl (Figure 3) that are additionally stabilized by intercalation. The 3R version is, in fact, evidently isostructural with 3R-Li_xMClH_y, M = Sc, Y.[13] The YClO substrate is the limiting structure achieved, starting with the partial, random occupancy of tetrahedral interstices found in the isostructural $ZrBrO_{0.3}$ and the related $ZrClO_{0.43}$ and $MClH_y$, M = Sc, Y. The family of interstitial derivatives of the ZrX structure types has also been expanded considerably in recent years through alternate occupation of octahedral sites within the four-layer slabs in 1T-type nitrides, carbides, and borides (Z) of formula M_2Cl_2Z, M = Sc, Y, Zr,[13,16,17] an hcp packing of the layers now providing the necessary relief from close approaches of Z and Cl along the c axis. The corresponding intercalates 1T-$M^I_xYClC_{0.5}$ are also known.[17]

An alternate view of the new phases reported herein is that they represent intercalation derivatives of the YOF form of YClO, especially for 3R-M_xYClO, which would be obtained by a direct expansion of that form of YClO and achieved for the postulated 1T-Cs_xYClO structure by simple slab displacement. Although the normal YClO structure is the tetragonal PbFCl type,[26] the production of the 3R (or YOF) type in this work by deintercalation led us to subsequent investigations and to the discovery that YOF-type MClO phases for M = Y, Ho, Er, and Tm could be obtained directly at lower temperatures by pyrohydrolysis of $(NH_4)_3MCl_6$ or by growth from melts.[23,37] The last three elements listed occur at the boundary of the transition from the normal (high-temperature) PbFCl form to SmSI-type structures for MClO. The SmSI structure is closely related to the YOF version and differs only in the stacking order for the four-layer slabs (SmSI:YOF as ZrCl:ZrBr in this sense), and indeed, intergrown samples of YOF and SmSI types are obtained in some of the

(37) The $(NH_4)_3YCl_6$ or like phases also react directly with Y_2O_3 or Y_2S_3 at 300–400 °C to form YClO or YClS in the YOF-type structure: Meyer, G.; Staffel, T.; Dötsch, S.; Schleid, T. *Inorg. Chem.*, in press.

low-temperature syntheses. The present 3R phases may then be viewed as the slightly less stable YOF-type structure for YClO stabilized through intercalation at 950 °C, the 2H- and 1T-type structures representing alternative arrangements that are not stable without intercalation since the alkali-metal atom lies between adjoining slabs in a trigonal-prismatic chlorine environment (Figure 3). In this connection, it is highly reasonable that the otherwise unknown (but not improbable) SmSI form of YClO was not found in an intercalated version since this would provide a less favorable environment for the alkali metal, namely, two yttrium atoms as second nearest neighbors along *c*.

We have been unsuccessful in accomplishing high-temperature intercalation reactions with PbFCl forms of RClO phases where a YOF-like structure is not stable, namely, with LaClO, NdClO, and GdClO. This must originate with the more compact PbFCl structure, which lacks a clear cleavage plane and contains instead square nets sequenced Cl–R–O–R–Cl with a ninth, strong R–Cl interaction across what otherwise could be a van der Waals gap.

The formation of only 3R-M^I_xYClO (or 1T-Cs_xYClO) when YOCl rather than Y_2O_3 and YCl_3 was reacted with MCl in the presence of yttrium (eq 2) is very reasonable in light of work by Beck,[38] who demonstrated and modeled the interconversion of structure types SmSI ⇄ YOF ⇄ PbFCl for ErClO through LuClO. (The YOF-type intermediate was generally not seen during his high-pressure experiments.) Similar conversions have been found to occur in fluxed reactions, where alkali-metal chlorides or MCl_3 generally favor the 3R type, whereas heat alone or YCl_3 gives the PbFCl type for YClO.[23] Thus, intercalation reactions run with preformed YClO in the PbFCl structure presumably proceed via the postulated direct transformation of the substrate to the YOF-type 3R-M^I_xYClO (or to 1T-Cs_xYClO) on intercalation. A reconstruction of the slabs would be required to achieve 2H-M^I_xYClO. Since the present work was completed, it has become evident[23] that the distribution of 2H- and 3R-type products obtained from MCl–YCl_3–Y_2O_3–Y reactions (eq 1) may, in fact, be determined by the course of a parallel or prior reaction of YCl_3 and Y_2O_3 to form YClO in the presence of different amounts of MCl. In addition, the observed decomposition of K_xYClO or YClO to Y_2O_3 for high KCl concentrations may result from the high relative stability of K_3YCl_6;[39] recrystallization of YClO from KCl in the absence of a reducing agent has been observed to give considerable decomposition to Y_2O_3 and Y_3O_4Cl as well as the 3R-YOF form.[23]

The present work also led to the discovery that 3R-RClO structures for R = Y, Ho, Er, Tm, and Yb could all be intercalated by sodium in liquid NH_3 at room temperature.[23] Only the yttrium product gave a reasonably sharp powder pattern, the *c* lattice constants obtained from separate experiments, 29.85 (5) and 30.07 (1) Å, comparing reasonably well with 29.947 (8) Å from the product of reaction 1 at 908 °C. Thus, reactions with *n*-butyllithium and sodium dithionate (Experimental Section) failed simply because these are too weak as reducing agents to affect intercalation of 3R-YClO.

Coordination of the Intercalated Metals. Rouxel et al.[40] have concluded that the coordination of intercalated alkali metal in transition-metal disulfides (MS_2) and in Ta_2S_2C is determined by three factors. The two most important factors are the size and amount of the intercalated atoms. The third factor concerns the nature of the M–S bond in systems with different transition metals and different chalcogens and does not apply to this investigation where the metal and halide remain the same. Their first observation is that smaller intercalated alkali-metal atoms exhibit trigonal-antiprismatic (TAP) coordination while larger atoms occur in a trigonal-prismatic (TP) arrangement. This can be understood by noting that with smaller alkali-metal atoms the adjoining nonmetal layers come closer together so that TAP coordination is obviously more favorable. Likewise, in the M_xYClO phases only 3R-Li_xYClO is observed with lithium where Li^+ is TAP. At the other extreme, both the more prevalent 2H- and 1T-Cs_xYClO phases involve TP cesium, and 3R-Cs_xYClO is converted to the 1T phase when annealed alone above 900 °C. The intermediate M^I = Na–Rb allows either the TP (2H) or the TAP (3R) coordination of M^I. The abnormally large lattice constant for 2H-Na_xYClO (Figure 1) may result from the borderline stability of the TP coordination at this point, the interslab Cl–Cl separation being about 3.60 Å.

One obvious factor correlating with this trend is the possible role of second nearest neighbor interactions across the gap. In the 3R structure of YCl, such Y··Cl interactions occur for all atoms (as in the ZrBr parent[3]), and these are retained in the 3R intercalates (but only as third neighbors) along with a gain from new second-neighbor M^I··O interactions (compare Figure 3a,b). The second attraction is retained in the 2H-type structure with TP coordination of M^I (Figure 3). Our model of the 1T-Cs_xYClO structure, Figure 4b; places TP cesium in an intermediate (acentric) position with one oxygen and one yttrium neighbor in the adjoining slabs. These "interpretations" are clearly simplistic in character, and a consideration of these interactions over more neighbors and greater distances would be better, relating as well to the as yet poorly understood differentiation between the ZrCl- and ZrBr-type parent structures.[3]

The second factor described by Rouxel and co-workers is that TAP coordination is generally favored as the alkali-metal concentration increases, as observed. This can be understood because the TAP arrangement places nonmetal atoms in adjoining slabs further apart as the reduction of host slabs increase. The advantage of this is emphasized by the extreme descriptions $M^+_x(MS_2)^{x-}$ and $M^+_x(YClO)^{x-}$.

Although the factors stated by Rouxel et al. for the intercalation of M^I in MS_2 appear to pertain to the M^I_xYClO phases, there are also some differences. In the sulfides only a single M^I appears to give structures with both TP and TAP coordination,[21,22] whereas for the M^I_xYClO phases this occurs for all M^I between sodium and cesium. A second difference is the absence of staged compounds in the present phases, which resemble the $M^I_xTa_2S_2C$[41] types in this respect. In the latter it is thought that the larger screening effect arising from five compound layers between alkali-metal galleries is responsible for the lack of staging,[22,41] and the same could be applicable here.

Hydrates. The hydrates $M^I_x(H_2O)_aYClO$ may be compared with the well-documented hydrates of the intercalated transition-metal disulfides, $M^I_x(H_2O)_aMS_2$.[21] Studies by Schöllhorn and Weiss[42,43] on the hydration properties of $M^I_xTiS_2$ and $M^I_xMoS_2$ have established the character of the ion- and solvent-exchange reactions and the existence of two clear hydration stages depending on cation hydration energy and water activity. The structure and bonding of the $M^I_x(H_2O)_aMS_2$ phases have been described by an ionic model in which the $(MS_2)^{x-}$ layers represent quasi, two-dimensional macroanions with delocalized negative charges, the interlayer space being occupied by solvated cations that are highly mobile at room temperature. As a consequence, these hydrates have typical polyelectrolyte character and undergo ion- and solvent-exchange reactions. Two structurally defined hydrate states are found for alkali-metal ions in the disulfides, corresponding to water monolayers, $\Delta c \sim 3$ Å, and bilayers $\Delta c \sim 6$ Å, where Δc is the increase in the *c* axis on hydration of each M^I layer. The formation of these structures depends on the cation hydration energy, with only the smaller cations, usually Li^+ and Na^+, having the capacity to form bilayers of water at sufficiently high activity. The single-crystal structures of two monolayer hydrates, $K_x(H_2O)_aTaS_2$ and $K_x(H_2O)_aNbS_2$ (with only the Nb or Ta and S positions refined), showed TP sites for the cation hydrate,[44] while a combined X-ray and neutron diffraction study of powdered bilayer hydrates indicate an expanded TAP site for

(38) Beck, H. P. *Z. Naturforsch., B: Anorg. Chem., Org. Chem.* **1977**, *32B*, 1015.
(39) Meyer, G. *Prog. Solid State Chem.* **1982**, *14*, 141.
(40) Rouxel, J.; Trichet, P.; Chevalier, P.; Colombet, P.; Ghalhoun, O. A. *J. Solid State Chem.* **1979**, *29*, 311.
(41) Brec, R.; Ritsma, J.; Ouvard, G.; Rouxel, J. *Inorg. Chem.* **1977**, *16*, 660.
(42) Schöllhorn, R.; Weiss, A. *Z. Naturforsch. B:* **1973**, *28B*, 71.
(43) Schöllhorn, R.; Weiss, A. *J. Less-Common Met.* **1974**, *36*, 229.
(44) Graf, H. A.; Lerf, A.; Schöllhorn, R. *J. Less-Common Met.* **1977**, *55*, 213.

the M^I hydrate.[45] Neutron diffraction and ^1H NMR studies place the oxygen in the plane of the alkali-metal layer with the two hydrogen atoms directed toward the sulfur layers in the monohydrates and toward another H_2O in the same plane and a sulfur layer in the bilayer.[21]

The most striking similarity between the hydration behavior of the intercalated disulfides and 2H-, 3R-K_xYClO and 3R-Rb_xYClO is the similarity of Δc in the latter, ~2.6 Å (Table II), and the evident trigonal-prismatic coordination of M^I (Figure 5). On this basis, we can probably conclude that the present phases also contain a monolayer of H_2O in trigonal-prismatic sites with the hydrogen atoms near the Cl layers. As with the hydrated dichalcogenides, the hydration-dehydration (3R-1T or 2H-2H) reactions of the chloride are reversible with the original YOCl phase being obtained on dehydration.

In the case of 3R-Li_xYClO, there is no hydration reaction in air, in contrast with Li_xMS_2 which forms bilayer hydrates, perhaps because the lattice energy with a more polar substrate is higher than the Li^+ hydration energy. The lithium salt was studied only at relatively low humidities, although liquid water was also without effect, while the behavior of the sodium compound was not investigated.

When the phases 3R-M^I_xYClO, M = Li-Cs and $x \simeq 0.1$-0.2, are placed in water, they are oxidized, as evidenced by the evolution of gas, and the crystals exfoliate. The $M^I_xMS_2$ phases for group 4 and 5 transition metals are evidently weaker reducing agents as they generally form crystalline hydrates and only reduce liquid water for x greater than 0.3-0.6.[46] When hydrogen is intercalated electrolytically into single crystals of 2H-TaS_2 in dilute acid, there is a large degree of exfoliation with no gas evolution.[47] The exfoliation in both cases is similar in appearance to the swelling observed in smectites or vermiculites and in particular the alkali-metal montmorillonites, $\sim M^I_x(Al,Mg)_4Si_8O_{20}(OH)_4 \cdot nH_2O$,[48] where the hydration is dominated by hydrogen bonding to the oxygen layers.

A "mechanism" for the exfoliation of 3R-M^I_xYClO may be postulated on the basis of visual evidence and the results for other systems. The first step is the hydration of M^I to form 1T-$M^I_x(H_2O)_aYClO$. This is followed by the oxidation of the slabs with loss of M^IOH and H_2 to give neutral (or lower charged) YClO slabs, perhaps with some decomposition. Some remaining water is hydrogen bonded to the chlorine layers. It is further hydration and hydrogen bonding within the interlayer region that causes the swelling or exfoliation. When these exfoliated "crystals" are removed from the water and mildly heated, most of the water evaporates and the "crystals" collapse back to plates. The plates must retain some water to allow the process to be repeatedly reversed, since the exfoliation cannot be repeated after the exfoliated "crystals" are dehydrated by heating. The phase at this point gives only very broad diffraction lines. In contrast, the 2H-M^I_xYClO phases, M = K or Rb, apparently form monolayer hydrates on exposure to moisture with no structural change as there are already TP sites available for H_2O. These 2H-type hydrates did not exfoliate or evolve H_2 in water.

The related 1T carbides, $M^I_xY_2Cl_2C$ with $x \simeq 1$ and M = Li, K, and Cs, have all been prepared, and the crystal structure confirmed with a single-crystal study of the potassium derivative. Both M^I and C occur in all TAP sites. These compounds decompose in moist air or water.[17] Intercalation of the analogous zirconium carbide phase has been unsuccessful, as is also true for the zirconium halide oxide and hydride analogues.

Acknowledgment. The authors are indebted to Prof. R. A. Jacobson and his group for continued X ray crystallographic services and to F. C. Laabs for the microprobe analyses.

Registry No. YClO, 13759-29-0; Y, 7440-65-5; Y_2O_3, 1314-36-9; NaCl, 7647-14-5; KCl, 7447-40-7; LiCl, 7447-41-8; CsCl, 7647-17-8; RbCl, 7791-11-9; sodium yttrium chloride oxide, 86993-42-2; potassium yttrium chloride oxide, 86993-37-5; lithium yttrium chloride oxide, 86993-32-0; cesium yttrium chloride oxide, 86993-29-5; rubidium yttrium chloride oxide, 86993-39-7.

Supplementary Material Available: Tables of the observed and calculated structure factor data for 2H-$K_{0.08}YClO$ and 3R-$Na_{0.08}YClO$ and the observed and calculated powder patterns for 1T-Cs_xYClO and 1T-$K_x(H_2O)_aYClO$ (4 pages). Ordering information is given on any current masthead page.

(45) Bos-Albernick, A. J. A.; Haange, R. J.; Wiegers, G. A. *J. Less-Common Met.* **1979**, *63*, 69.
(46) Schöllhorn, R. In "Intercalation Chemistry"; Whittingham, M. S., Jacobson, A. J., Eds., Academic Press: New York, 1982; p 324.
(47) Murphy, D. W.; Hull, C. W. *J. Chem. Phys.* **1975**, *62*, 973.
(48) Grim, R. F. "Clay Mineralogy"; McGraw-Hill: New York, 1968.

Contribution from the Department of Chemistry, Gorlaeus Laboratories, State University Leiden, 2300 RA Leiden, The Netherlands

Magnetic Properties of Dimeric Disubstituted-Triazole Copper(II) Compounds. X-ray Structure of Bis[μ-3,5-bis(pyridin-2-yl)-1,2,4-triazolato-N',N^1,N^2,N']-bis[aqua(trifluoromethanesulfonato-O)copper(II)]

ROB PRINS, PAUL J. M. W. L. BIRKER, JAAP G. HAASNOOT,* GERRIT C. VERSCHOOR, and JAN REEDIJK

Received February 13, 1985

The crystal and molecular structure of bis[μ-3,5-bis(pyridin-2-yl)-1,2,4-triazolato-N',N^1,N^2,N']bis[aqua(trifluoromethanesulfonato-O)copper(II)] ($[Cu(bpt)(CF_3SO_3)(H_2O)]_2$, bpt = $C_{12}N_5H_8^-$) was determined by X-ray diffraction methods. Crystal data: triclinic, centrosymmetric, space group $P\bar{1}$ with a = 8.841 (3) Å, b = 14.131 (6) Å, c = 14.392 (6) Å, α = 112.58 (3)°, β = 92.23 (3)°, γ = 102.45 (3)°, Z = 2, and V = 1606 (1) Å^3. The least-squares refinement based on 2832 significant reflections converged at R = 0.023 and R_w = 0.025. The structure consists of dimeric units $[Cu_2L_2]^{2+}$ with a copper-copper distance of 4.085 (1) Å. Each symmetry-independent CuN_4O_2 chromophore in the dimer is a six-coordinate distorted octahedron. The oxygen donor ligands are a water molecule and a triflate anion. The Cu atoms in the dimer are bridged by two triazole rings. The magnetic susceptibility measurements show quite large antiferromagnetic interactions with a singlet-triplet splitting of 204-236 cm^{-1} between the metal centers in a series of isostructural copper(II) compounds with the anions NO_3^-, ClO_4^-, BF_4^-, and $CF_3SO_3^-$. Strong magnetic interactions in these compounds having a singlet ground state was also evident from the temperature dependence of the intensity of the excited triplet state as observed in powder EPR spectra. In addition the powder EPR spectrum of the title compound revealed copper hyperfine interactions at 77 K.

Introduction

The magnetic properties of paramagnetic transition-metal ions incorporated in various coordination compounds have been the subject of intensive study over the past decades. The best known examples are dinuclear copper(II) compounds. Useful correlations between the singlet-triplet splitting, which is mainly determined by the exchange interaction between ground-state magnetic orbitals, and structural parameters have been made.[1-3] Another

(1) Hodgson, D. J. *Prog. Inorg. Chem.* **1975**, *19*, 173.

0020-1669/85/1324-4128$01.50/0